RESEARCH ARTICLE

Association of Cortical and Subcortical Microstructure With Clinical Progression and Fluid Biomarkers in Patients With Parkinson Disease

Linbo Wang, PhD,* Cheng Zhou, MD,* Wei Zhang, MSc, Minming Zhang, MD,† Wei Cheng, PhD,† and Jianfeng Feng, PhD†

Correspondence
Dr. Feng
jffeng@fudan.edu.cn

Neurology® 2023;101:e300-e310. doi:10.1212/WNL.0000000000207408

Abstract

Background and Objectives

Mean diffusivity (MD) of diffusion MRI (dMRI) has been used to measure cortical and subcortical microstructural properties. This study investigated relationships of cortical and subcortical MD, clinical progression, and fluid biomarkers in Parkinson disease (PD).

Methods

This longitudinal study using data from the Parkinson's Progression Markers Initiative was collected from April 2011 to July 2022. Clinical symptoms were assessed with Movement Disorder Society–sponsored revision of the Unified Parkinson's Disease Rating Scale (UPDRS) and Montreal Cognitive Assessment (MoCA) scores. Clinical assessments were followed up to 5 years. Linear mixed-effects (LME) models were performed to examine associations of MD and the annual rate of changes in clinical scores. Partial correlation analysis was conducted to examine the associations of MD and fluid biomarker levels.

Results

A total of 174 patients with PD (age 61.9 ± 9.7 years, 63% male) with baseline dMRI and at least 2 years of clinical follow-up were included. Results of LME models revealed a significant association between MD values, predominantly in subcortical regions, temporal lobe, occipital lobe, and frontal lobe, and annual rate of changes in clinical scores (UPDRS-Part-I, standardized $\beta > 2.35$; UPDRS-Part-II, standardized $\beta > 2.34$; postural instability and gait disorder score, standardized $\beta > 2.47$; MoCA, standardized $\beta < -2.42$; all $p < 0.05$, false discovery rate [FDR] corrected). In addition, MD was associated with the levels of neurofilament light chain in serum ($r > 0.22$) and α-synuclein (right putamen $r = 0.31$), β-amyloid 1–42 (left hippocampus $r = -0.30$), phosphorylated tau at 181 threonine position ($r > 0.26$), and total tau ($r > 0.23$) in CSF at baseline (all $p < 0.05$, FDR corrected). Furthermore, the β coefficients derived from MD and annual rate of changes in the clinical score recapitulated the spatial distribution of dopamine (DAT, D1, and D2), glutamate (mGluR5 and NMDA), serotonin (5-HT_{1a} and 5-HT_{2a}), cannabinoid (CB1), and γ-amino butyric acid A receptor neurotransmitter receptors/transporters ($p < 0.05$, FDR corrected) derived from PET scans in the brain of healthy volunteers.

Discussion

In this cohort study, cortical and subcortical MD values at baseline were associated with clinical progression and baseline fluid biomarkers, suggesting that microstructural properties could be useful for stratification of patients with fast clinical progression.

*These authors contributed equally to this work.

†These authors contributed equally to this work as senior authors.

From the Institute of Science and Technology for Brain-Inspired Intelligence (L.W., W.Z., W.C., J.F.), Fudan University; Key Laboratory of Computational Neuroscience and Brain-Inspired Intelligence (Fudan University) (L.W., W.Z., W.C., J.F.), Ministry of Education; MOE Frontiers Center for Brain Science (L.W., W.Z., W.C., J.F.), Fudan University; Zhangjiang Fudan International Innovation Center (L.W., W.Z., W.C., J.F.), Shanghai; Department of Radiology (C.Z., M.Z.), The Second Affiliated Hospital, Zhejiang University School of Medicine, Hangzhou; Fudan ISTBI—ZJNU Algorithm Centre for Brain-inspired Intelligence (W.C.), Zhejiang Normal University, Jinhua, China; and Department of Computer Science (J.F.), University of Warwick, Coventry, United Kingdom.

Go to Neurology.org/N for full disclosures. Funding information and disclosures deemed relevant by the authors, if any, are provided at the end of the article.

Glossary

3D = 3 dimensional; **5-HT$_{1a}$** = 5-hydroxytryptamine receptor subtype 1a; **Aβ42** = β-amyloid 1–42; **CB1** = cannabinoid type 1 receptor; **dMRI** = diffusion tensor MRI; **D1** = dopamine receptor 1; **D2** = dopamine receptor 2; **DAT** = dopamine transporter; **FDR** = false discovery rate; **GABA** = γ-amino butyric acid A receptor; **GO** = gene ontology; **GSEA** = gene set enrichment analysis; **H3** = histamine H3 receptors; **LEDD** = levodopa equivalent daily dose; **LME** = linear mixed effects; **MD** = mean diffusivity; **UPDRS** = Unified Parkinson's Disease Rating Scale; **MNI** = Montreal Neurological Institute; **MoCA** = Montreal Cognitive Assessment; **MOR** = mu opioid receptor; **mRNA** = messenger RNA; **NET** = noradrenaline transporter; **NfL** = neurofilament light; **NMDA** = N-methyl D-aspartate receptor; **PAP** = progression-associated pattern; **PD** = Parkinson disease; **PIGD** = postural instability and gait disorder; **PPMI** = Parkinson's Progression Markers Initiative; **p-tau181** = phosphorylated tau at 181 threonine position; **SNc** = substantia nigra pars compacta; **SOMAmers** = slow off-rate modified aptamers; **TE** = time to echo; **TR** = repetition time; **t-tau** = total tau; **VAChT** = vesicular acetylcholine transporter.

Parkinson disease (PD) is characterized by the abnormal accumulation of pathologic α-synuclein in the midbrain substantia nigra pars compacta (SNc) that leads to dopaminergic neuron loss.[1-5] Axonal degeneration caused by pathologic α-synuclein aggregates precedes neuron loss in the pathogenesis of PD.[3,4,6] And, α-synuclein strains can target distinct brain regions through cell-to-cell spreading of protein aggregates.[2,7] Therefore, axonal degeneration caused by pathologic α-synuclein aggregates may occur in areas of the nervous system beyond the SNc in the absence of neuronal loss.[2,4]

Diffusion tensor MRI (dMRI) diffusivity measurements are useful biomarkers in monitoring axonal damage.[8] The mean diffusivity (MD) value of dMRI, a quantitative measure of the mean motion of water molecules, has been used mainly to describe microstructural properties in the white matter.[4,9,10] However, the MD value can also be used to detect microstructural properties in the gray matter because the motion of water molecules in gray matter is nearly isotropic.[11-13] An increased MD value in the gray matter is thought to reflect microstructural disorganization because of damage to dendritic processes or cellular membranes that led to fewer obstacles to diffusion; therefore, water molecules are able to diffuse more freely.[11,12] An increased MD value in the gray matter has been proposed as a sensitive biomarker of microstructural alterations that might predate macrostructural atrophy (i.e., gray matter volume loss).[14,15]

In PD, increased MD values have been reported in the white matter and gray matter at the time of diagnosis.[13] Moreover, MD values of the white matter and temporo-occipital region are associated with in vivo levels of neurofilament light (NfL) in PD, which is a sensitive measurement of neuroaxonal damage.[16-18] In addition, MD values of the white matter and globus pallidus (pallidum) are associated with worsening of motor severity and cognitive decline in patients with PD.[9,10,19] However, the relationship between MD values of the cortex and other subcortical regions beyond basal ganglia and clinical progression and its relationships with the in vivo levels of α-synuclein, β-amyloid, and tau in patients with PD remain to be determined.

Most previous research on the relationship between diffusivity measurements and clinical progression in PD has focused on the white matter.[10,19,20] This study focused on cortical and subcortical MD values in the gray matter to investigate its relationship with clinical progression and fluid biomarkers. Although the cardinal motor symptoms of PD are a consequence of progressive dopaminergic neuron loss in the SNc,[21] many other neurotransmitter systems can be affected and involved in the etiology of PD symptoms.[5,22] Therefore, we investigated the spatial correlation between the progression-associated pattern derived from MD and clinical progression and the spatial distribution of neurotransmitter receptors/transporters to uncover specific neurotransmitter links. The hypotheses being tested were that baseline microstructural alterations of PD are associated with clinical progression and fluid biomarkers for neurodegeneration and occur in association with the availability of specific neurotransmitter receptors/transporters in the brain of healthy controls.

Methods

Participants

Participants in this study were recruited from the Parkinson's Progression Markers Initiative (PPMI).[23,24] The PPMI is a prospective, longitudinal, observational multicenter study that aims to identify biomarkers of PD.[23,24] The inclusion criteria for patients with PD in the PPMI were (1) 30 years or older, (2) within 2 years of diagnosis, (3) baseline Hoehn and Yahr stage less than III, (4) dopaminergic deficit on imaging, (5) untreated with dopamine replacement therapy, and (6) have either at least 2 of rigidity, resting tremor, or bradykinesia (must have either bradykinesia or resting tremor) or a single asymmetric bradykinesia or asymmetric resting tremor.[23] Patients with PD received evaluations of motor function at baseline, every 3 months during the first year, and every 6 months during the subsequent 4 years (eTables 1 and 2, links.lww.com/WNL/C827) and received evaluations of nonmotor function at baseline and every year during the subsequent 4 years. Only patients with baseline 3-dimensional (3D) T1-weighted MRI, dMRI, and at least 2 years of clinical follow-up were included in this study. Therefore, 174 patients with PD were included (Table 1). A flowchart of patient selection is shown in eFigure 1.

Table 1 Baseline Characteristics of the Study Participants

Characteristics	PD (n = 174)
Age, y	61.87 (9.65)
Male sex, n (%)	109 (63)
Race White, n (%)	169 (97)
Education, y	15.56 (2.93)
Disease duration, y	0.84 (1.18)
UPDRS scores	
Part-I	5.48 (4.38)
Part-II	5.67 (4.43)
Part-III	21.10 (9.44)
PIGD	0.23 (0.23)
Tremor	0.46 (0.33)
Cognitive scores	
Montreal Cognitive Assessment	27.49 (2.05)
Benton Judgment of Line Orientation	12.62 (2.25)
Hopkins Verbal Learning Test total recall	24.88 (5.24)
Letter-Number Sequencing	10.78 (2.76)
Semantic Fluency Test	48.02 (11.35)
Symbol Digit Modalities Test	41.60 (10.03)
Fluid biomarkers	
Serum NfL, pg/mL	12.48 (6.28)
CSF α-synuclein, pg/mL	1477.38 (702.81)
CSF $A\beta_{42}$, pg/mL	857.62 (343.43)
CSF p-tau181, pg/mL	14.44 (4.97)
CSF t-tau, pg/mL	166.27 (54.38)

Abbreviations: $A\beta_{42}$ = β-amyloid 1–42; UPDRS = Movement Disorder Society–sponsored revision of the Unified Parkinson's Disease Rating Scale; NfL = neurofilament light; PD = Parkinson disease; PIGD = postural instability and gait disturbance subscale of UPDRS; p-tau181 = phosphorylated tau at threonine 181; t-tau = total tau; tremor = tremor subscale of UPDRS.
Values are presented as mean (SD). All patients with PD were untreated with PD medications at baseline assessment.

Standard Protocol Approvals, Registrations, and Patient Consents

The study was approved by the local ethics committees of the participating sites. Written informed consent was obtained from all patients participating in the study.

Baseline and Follow-up Clinical Assessments

Demographic characteristics, including age, sex, race, level of education, and disease duration, were recorded at baseline (Table 1 and eTable 3, links.lww.com/WNL/C827). Motor and nonmotor assessments included Movement Disorder Society–sponsored revision of the Unified Parkinson's Disease Rating Scale (UPDRS),[25] including UPDRS-Part-I, UPDRS-Part-II, UPDRS-Part-III, and 2 motor subscales for postural instability and gait disorder (PIGD) and tremor. The PIGD subscale was calculated as the mean of 5 items, including walking, balance and freezing in UPDRS part II (item 2.12 and 2.13), gait, and postural stability and freezing of gait in UPDRS part-III (item 3.10, 3.11, and 3.12); the tremor subscale was calculated as the mean of 11 items, including tremor in UPDRS-II (item 2.10) and postural tremor, kinetic tremor, rest tremor, and rest constancy in UPDRS-III (item 3.15–3.18). At baseline, patients were untreated with PD medications.[23,24] However, they initiate PD medications after enrollment at the time that the patient or investigator deemed it clinically necessary.[23,24] Therefore, UPDRS-Part-III of follow-up visits were assessed on 2 occasions: OFF and ON their usual dose of medication.[23,24] At OFF visits, patients were asked to withdrawal their dopaminergic medication 6–12 hours before the UPDRS Part-III assessment. After this assessment, patients were asked to take their usual dose of medication, and a second UPDRS Part-III motor assessment was performed at least 1 hour after dosing in the clinic. The levodopa equivalent daily dose (LEDD) scores were calculated for each patient and each visit (eTable 1).[26] The Montreal Cognitive Assessment (MoCA) was used to assess global cognition.[27] Cognitive testing also included the Hopkins Verbal Learning Test total recall to assess verbal learning and memory,[28] Symbol Digit Modalities Test to assess cognitive processing speed,[29] Benton Judgment of Line Orientation Test to assess visuospatial function,[30] and Letter-Number Sequencing to assess attention and working memory.[31]

MRI Acquisition and Processing

All participants included in this study underwent a structural 3D T1-weighted MRI and dMRI on Siemens 3.0 T scanner from different participating sites. The scanning parameters of 3D T1-weighted MRI were as follows: repetition time (TR) = 2,300 milliseconds; time to echo (TE) = 2.98 milliseconds; inversion time = 900 milliseconds; flip angle = 90°; slice number = 176; acquisition matrix = 240 × 256, and voxel size = 1 × 1 × 1 mm^3. The diffusion tensor image was obtained with the following parameters: TR = 900 milliseconds, TE = 88 milliseconds, flip angle = 90°, voxel size = 2 × 2 × 2 mm^3, slice number = 72, and 64 gradient directions with a b value of 1,000 s/mm^2. One nongradient volume (b = 0 s/mm^2) was also acquired.

dMRI data were processed using FMRIB's Software Library (version 5.0.9). Data were first skull stripped and then corrected for eddy current distortions and motion effects using EDDY. Then, diffusion tensors were fitted, and MD maps were generated using DTIFIT. The cortical MD values were extracted on the cortical skeleton using the following steps that can mitigate partial volume effects.[12] First, nonbrain tissues were removed from each participant's T1-weighted image. Next, each native non–diffusion-weighted (B = 0) image was linearly aligned to the skull-stripped T1-weighted image. Then, field bias correction, gray matter segmentations, and affine and

nonlinear registration were conducted on each T1-weighted image. Fourth, the normalized gray matter probability maps of all patients were used to create a median gray matter skeleton with a threshold of 0.2 to minimize the contribution of voxels from the white matter and CSF that can confound the cortical MD measures. Fifth, native MD maps were normalized into the Montreal Neurological Institute (MNI) standard space by using the registration information of the T1-weighted image and projected onto the median gray matter skeleton. Finally, the regional MD values were extracted according to the boundaries and labeling of the Desikan-Killiany atlas.

Because PD pathologic changes occur early in subcortical regions,[2,3,32] MD values of subcortical regions (i.e., caudate, putamen, thalamus, pallidum, hippocampus, amygdala, and nucleus accumbens) were also extracted for subsequent analysis. The B0 images were registered to an individual T1-weighted image using the boundary-based registration (bbregister tool) in FreeSurfer 6.0, as a previous study.[33] Average MD values were extracted for each subcortical region after aligning the MD maps into T1-weighted space using the B0 image-derived registration parameters.[33]

PET Data Acquisition

We used previously curated density maps of 19 receptors and transporters across 9 different neurotransmitter systems.[34] These neurotransmitter density maps were derived from PET or SPECT from the brain of different groups of healthy individuals, covering the following neurotransmitter systems: dopamine (D1, D2, FDOPA, and DAT), glutamate (mGluR5), serotonin (5-HT_{1a}, 5-HT_{1b}, 5-HT_{2a}, 5-HT_{4}, 5-HT_{6}, and 5-HTT), γ-amino butyric acid A receptor (GABA) ($GABA_{A/BZ}$), endocannabinoids (CB1), noradrenaline (NET), acetylcholine (α4β2, M1, and VAChT), opioids (MU), and histamine (H3).[34] Details of each receptor/transporter, corresponding PET or SPECT tracer, number of healthy individuals, age, and sex of each scan can be found in eTable 4 (links.lww.com/WNL/C827). All PET and SPECT images were registered to the MNI-ICBM 152 nonlinear atlases (version 2009). Each tracer map corresponding to each receptor/transporter was derived from the average group of different healthy individuals. Then, each tracer map was parcellated into the Desikan-Killiany atlas and z-scored across regions.

Fluid Biomarker Measurements

Collection, handling, shipment, and storage of CSF and blood samples were implemented according to the PPMI biologic manual.[23] Both CSF and blood samples included in this study were collected at baseline.

The Simoa singleplex NF-light assay was used for the measurements of NfL protein in serum. The measurements of α-synuclein in CSF were analyzed by using an ELISA kit commercially available from BioLegend. Measurements of β-amyloid 1–42 ($A\beta_{42}$), phosphorylated tau at threonine 181 position (p-tau181), and total tau (t-tau) in CSF were obtained by using the multiplex Luminex xMAP platform with research-use-only Fujirebio-Innogenetics INNO-BIA AlzBio3 immunoassay kit-based reagents.

Proteomics data from CSF of patients with PD were quantified using the SOMAscan platform, which is based on protein-capture slow off-rate modified aptamers (SOMAmers) molecules with high affinity and specificity.[35] The proteomics data are controlled for quality to remove outlier samples, calibrators, buffer, and nonhuman SOMAmers. The measured values are hybridization-normalized, plate-scaled, median-normalized intraplate and calibrated at SomaLogic's side, then log2 transformed, median-normalized interplates, and batch corrected at the plate level. Batch effects were removed by applying "ComBat" using an empirical Bayes method.[36]

Functional Enrichment Analysis

To investigate the possible underlying mechanism of microstructural changes that associated with clinical progression, gene set enrichment analysis (GSEA)[37] was performed for CSF proteins associated with MD. The partial Spearman rank correlation was performed between the MD value and CSF protein levels with adjustment for sex, age, years of education, race, and study site. In these correlation analyses, we used the MD value of brain regions that have MD values significantly associated with a longitudinal change in 1 or more clinical scores (i.e., UPDRS-Part-I, UPDRS-Part-II, PIGD, and MoCA). CSF proteins were then ranked in a descending order according to its correlation coefficients with the MD value. GSEA was performed using the *clusterProfiler*[38] package by fed into the list of ranked CSF proteins.

Statistical Analysis

Linear mixed-effects (LME) models were used to examine the association of baseline MD values with the annual rate of changes in clinical scores using disease duration as the time scale. We separately built LME models between each regional MD value and each clinical score, where each regional MD value and its interaction with time were used as independent variables, and each clinical score was used as a dependent variable. Confounding variables including age, sex, race (categorized as White or others), education, and study site were adjusted as fixed effects in these LME models with random intercept and slope for each patient. All follow-up points were used for this longitudinal analysis, and missing data of follow-up visits were not included. Disease duration was computed as the time from clinical diagnosis.[23,24] Because medication can have a profound effect on disease course, we estimated the correlations of MD and the annual rate of changes in UPDRS-Part-III in the dopaminergic ON state separately for treated periods, with added time-varying LEDD as fixed effects in the LME model. Hereafter, we will refer to the regional β coefficients derived from MD values and the annual rate of changes in clinical scores as progression-associated pattern (PAP).

Partial Spearman rank correlations were performed to test the baseline relationship of MD values and fluid biomarker levels with adjustment for covariates, including sex, age, years of education, race, and study site. All the region-wise analyses

Figure 1 Correlation Between Baseline MD Values and the Annual Rate of Changes in the Clinical Score

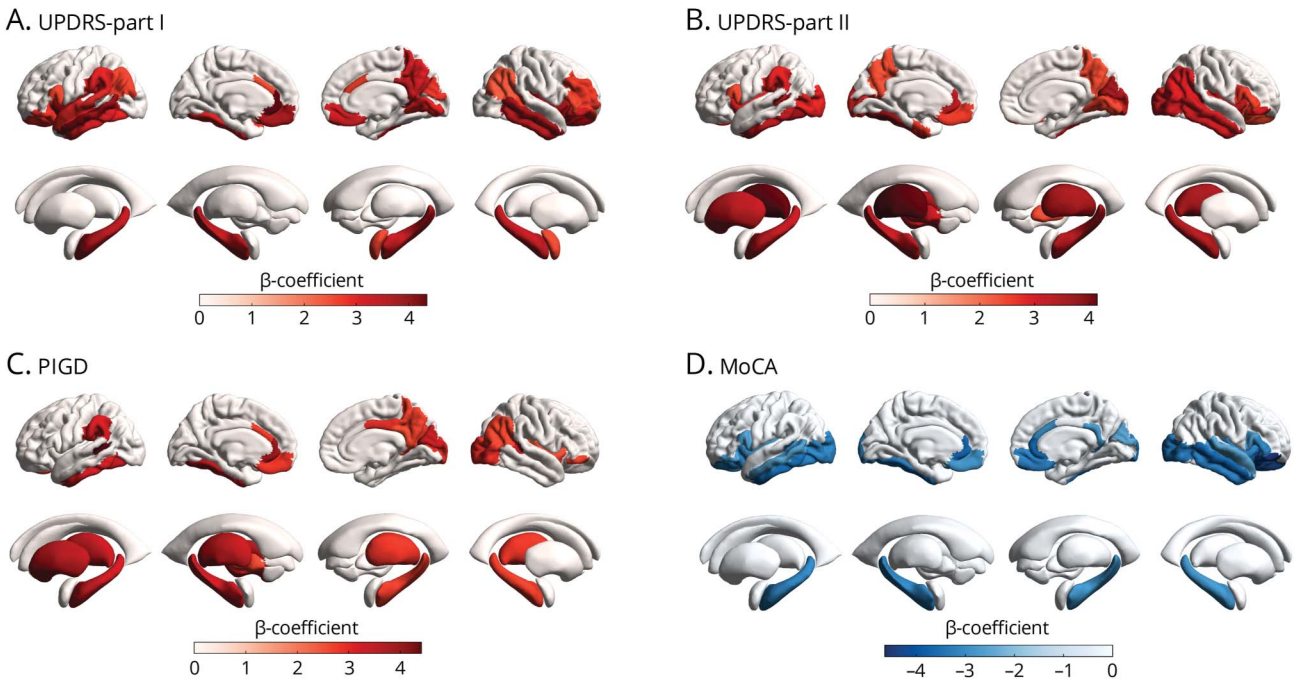

Color bars indicate standardized β coefficients for the interaction of MD and disease duration on longitudinal deterioration of UPDRS-Part I (A), UPDRS-Part II (B), PIGD score (C), and MoCA (D). Regions shown have a p value of <0.05 after FDR correction for multiple comparisons. FDR = false discovery rate; MD = mean diffusivity; UPDRS = Movement Disorder Society–sponsored revision of the Unified Parkinson's Disease Rating Scale; MoCA = Montreal Cognitive Assessment; PIGD = postural instability and gait disorder.

described above were corrected for multiple comparisons across 86 Desikan-Killiany regions by using the Benjamini-Hochberg false discovery rate (FDR) correction. Spearman rank correlations were also performed to test the association between PAPs of each clinical score and the neurotransmitter density map of each receptor/transporter, with p-value correction for multiple comparisons (19 neurotransmitter receptors/transporters) using the FDR. Demographic and clinical variables were reported as mean (SD). All tests were 2-sided with a significance level of $p < 0.05$.

Data Availability

Data used in the preparation of this article were obtained from the PPMI database (ppmi-info.org/data). For up-to-date information on the study, visit ppmi-info.org.

Results

Demographics and Clinical Variables

Clinical and demographic data of patients with PD are summarized in Table 1. At baseline, patients with PD were newly diagnosed and untreated with dopamine replacement therapy, the mean (SD) age of patients with PD (n = 174) was 61.87 (9.65) years, the mean (SD) disease duration of diagnosis was 0.84 (1.18) years, the percentage of female was 37%, and the percentage of male was 63%. The mean (SD) disease duration between diagnosis date and the last study visit of patients with PD was 5.82 (1.20) years. In LME models controlling for covariates, the severity of UPDRS Parts I, II, and III, PIGD, and tremor was increased by approximately 0.98 (95% CI 0.09–10.46), 1.10 (95% CI 0.10–11.16), 2.04 (95% CI 0.23–9.06), 0.07 (95% CI 0.01–6.67), and 0.02 (95% CI 0.01–2.65) units per year, and the MoCA score was decreased by approximately 0.17 (95% CI −0.05 to 3.21) units per year (eTable 5, links.lww.com/WNL/C827).

Correlations Between Baseline MD Values and Clinical Progression

Baseline MD values correlated with the annual rate of changes in the clinical score were observed primarily in subcortical regions, temporal lobe, occipital lobe, and frontal lobe ($p <$ 0.05, FDR corrected; Figure 1). Specifically, higher MD values correlated with a faster increase in UPDRS-Part-I were most prominent in the left rostral anterior cingulate, left insula, right insula, left middle temporal, left medial orbitofrontal, and right middle temporal (Figure 1A). Higher MD values correlated with a faster increase in UPDRS-Part-II were most prominent in the left thalamus, left fusiform, right thalamus, right cuneus, and right insula (Figure 1B). Higher MD values correlated with a faster increase in PIGD were most prominent in left banks of the superior temporal sulcus, left rostral anterior cingulate, left cerebellum, left fusiform, and left putamen (Figure 1C, eTable 6, links.lww.com/WNL/C827). Particularly, higher MD values in the left pallidum and putamen were associated with a faster increase in UPDRS-Part-II and PIGD (Figure 1, B and C). The correlations between

Figure 2 Correlation Between MD Values and Serum and CSF Biomarkers at Baseline

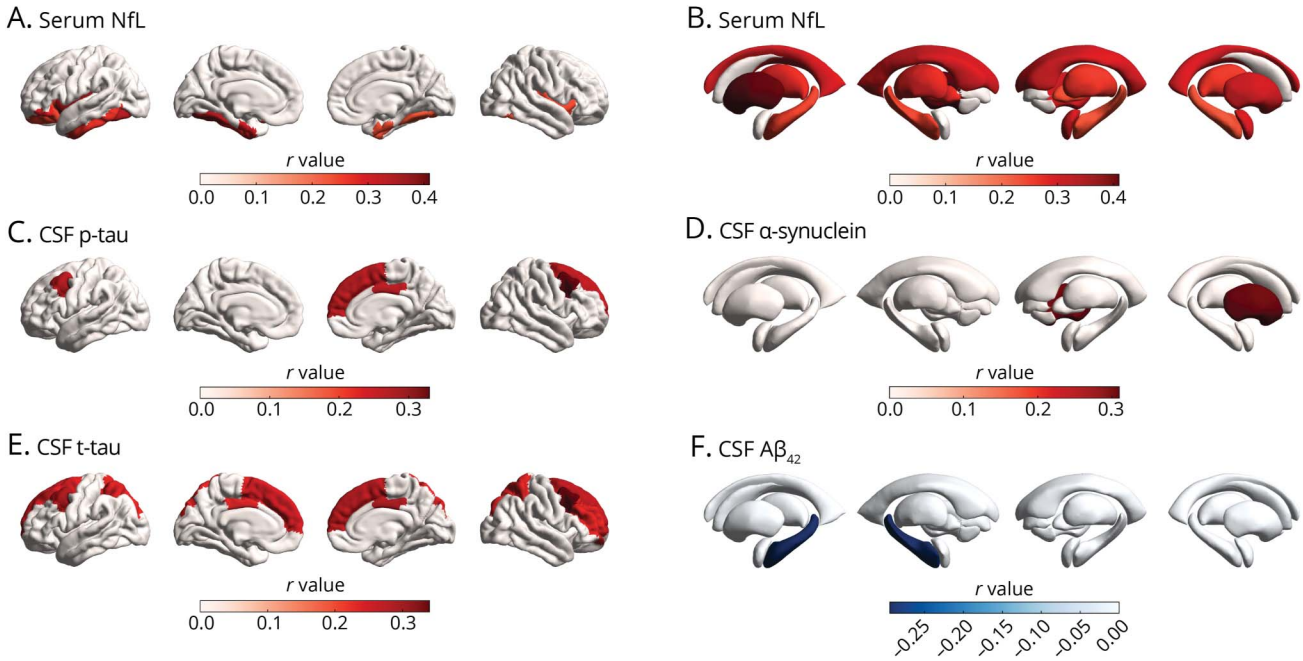

Color bars indicate Spearman correlation coefficients for the correlation of MD and serum NfL (n = 143) (A, B), CSF p-tau181 (n = 159) (C), CSF α-synuclein (n = 163) (D), CSF t-tau (n = 166) (E), and CSF $A\beta_{42}$ (n = 160) (F). Regions shown have a p value of <0.05 after FDR correction for multiple comparisons. $A\beta_{42}$ = β-amyloid 1–42; FDR = false discovery rate; MD = mean diffusivity; NfL = neurofilament light; p-tau181 = phosphorylated tau at threonine 181; t-tau = total tau.

baseline MD values and the annual rate of changes in UPDRS-Part-III in the dopaminergic OFF state and tremor did not survive FDR correction. However, some temporal, occipital, and subcortical MD values were correlated with the annual rate of changes in UPDRS-Part-III in the dopaminergic ON state after FDR correction (eFigure 2).

Higher MD values were associated with a faster decline in MoCA in the right pars orbitalis, right lateral orbitofrontal, left rostral anterior cingulate, right middle temporal, and right rostral anterior cingulate (Figure 1D). In subanalysis, we also found that cortical and subcortical MD values were associated with longitudinal changes in the domain-specific cognitive score, including Hopkins Verbal Learning Test total recall, Semantic Fluency Test, and Symbol Digit Modalities Test (eFigure 3 and eTable 7, links.lww.com/WNL/C827).

Correlations Between MD Values and Fluid Biomarker Levels at Baseline

Next, we investigated the baseline correlations of MD values with levels of serum and CSF biomarkers in patients with PD. The MD value of regions that showed positive correlations with serum NfL levels was located predominantly in subcortical regions and the temporal lobe ($p < 0.05$, FDR corrected; Figure 2, A and B, eTable 8, links.lww.com/WNL/C827). The MD value of regions that showed positive correlations with CSF p-tau181 and t-tau levels was primarily in the frontal lobe and parietal lobe ($p < 0.05$, FDR corrected; Figure 2, C and E, eTable 8). The MD value of the right putamen was positively correlated with the CSF α-synuclein level ($\beta = 0.31$, $p < 0.05$, FDR corrected; Figure 2D). The MD value of the left hippocampus was negatively correlated with the CSF $A\beta_{42}$ level ($\beta = -0.30$, $p < 0.05$, FDR corrected; Figure 2F). The correlations between cortical MD values and CSF α-synuclein levels and CSF $A\beta_{42}$ levels did not survive FDR correction.

Enrichment Analysis of CSF Proteins Associated With MD

Gene ontology (GO) enrichment analyses were applied to the CSF proteins listed in the descending order according to its correlation coefficients with the MD value of regions that significantly correlated with the annual rate of changes in clinical scores (eFigure 4A, links.lww.com/WNL/C827). The significant GO terms for top of the ordered CSF protein list included messenger RNA (mRNA) metabolic process, DNA binding, chromosome organization, nuclear protein-containing complex, cytoskeleton, and mitochondrion, which are intracellular components or biological processes (eFigure 4B). The significant GO terms for bottom of the ordered CSF protein list included axon guidance, neuron differentiation, cell morphogenesis, CNS development, presynaptic membrane organization, forebrain development, and head development, which are related to biological processes of neuron development (eFigure 4C). In addition, the significant GO terms for bottom of the ranked list of CSF protein included glycoprotein-related process, Golgi membrane, lysosomal lumen, and transmembrane receptor tyrosine kinase activity (eFigure 4C).

Figure 3 Spatial Correlation Analyses Between PAPs and Neurotransmitter Density Maps

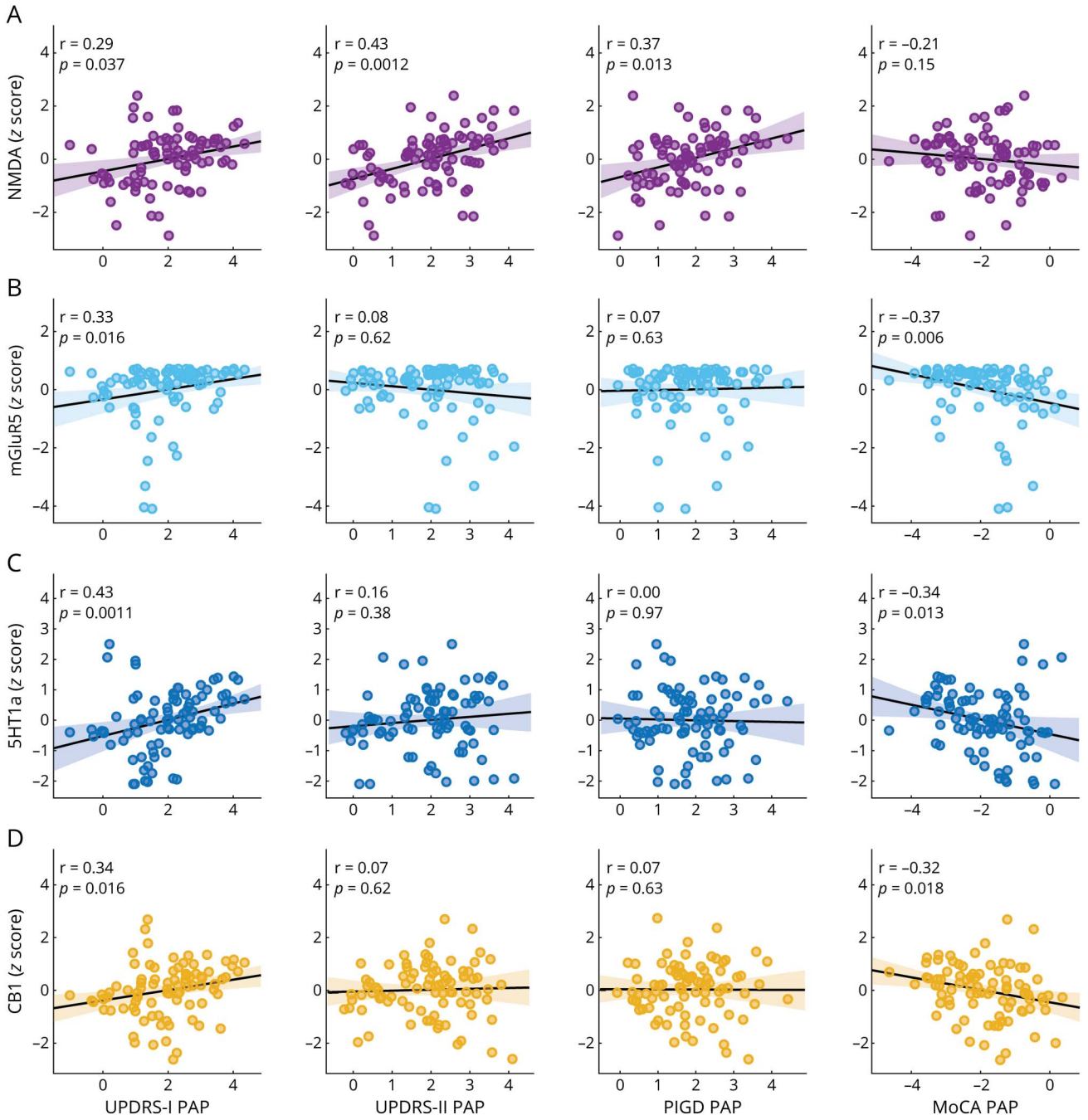

Spatial correlations of PAPs with NMDA (A), mGlu5 (B), 5-HT1a (C) and CB1(D) density maps. Spearman correlation coefficients and *p* values (FDR corrected) are displayed. 5-HT_{1a} = 5-hydroxytryptamine receptor subtype 1a; CB1 = cannabinoid type 1 receptor; UPDRS = Unified Parkinson's Disease Rating Scale; mGlu5 = metabotropic glutamate type 5 receptor; NMDA = N-methyl D-aspartate receptor; PAP = progression-associated pattern; PIGD = postural instability and gait disorder.

Correlations Between PAPs and Spatial Distribution of Neurotransmitter Receptors/Transporters

We therefore sought to relate PAPs of MD to spatial distribution of neurotransmitter receptors/transporters. Figure 3 and eFigures 5–8 show how neurotransmitter distribution maps onto PAPs across 4 clinical scores. We found that UPDRS-II PAP was positively correlated with the distribution of dopaminergic receptors/transporters, including DAT and D2, and UPDRS-I PAP was positively correlated with the distributions of D1 ($p < 0.05$; FDR corrected; eFigure 5, links.lww.com/WNL/C827). Furthermore, the distribution maps of the glutamate receptor were correlated with PAPs of UPDRS-I (NMDA and $mGluR_5$), UPDRS-II (NMDA), PIGD (NMDA), and MoCA ($mGluR_5$) ($p < 0.05$; FDR corrected; Figure 3, A and B). In addition, we found that both serotonin

receptor (5-HT_{1a}) distributions and cannabinoid receptor (CB1) distributions were related to PAPs of UPDRS-I and MoCA ($p < 0.05$; FDR corrected; Figure 3, C and D). Finally, MoCA PAP was related to the spatial distribution of 5-HT_{2a} and GABA ($p < 0.05$; FDR corrected; eFigures 6 and 8). The associations between spatial distribution of neurotransmitter receptors/transporters and PAPs were similar for the whole brain and cortical regions (eTable 9).

Discussion

In this study, we found that higher MD values, predominantly in subcortical regions, temporal lobe, occipital lobe, and frontal lobe, were associated with faster progression of motor and nonmotor symptoms in PD. In addition, baseline MD values were associated with fluid biomarkers (i.e., NfL in serum and α-synuclein, $A\beta_{42}$, p-tau181, and t-tau in CSF). Furthermore, we found that PAPs were associated with the spatial distribution of dopamine, glutamate, serotonin, cannabinoids, and GABA neurotransmitters of healthy volunteers. Altogether, our findings suggest that higher MD values in subcortical regions, temporal lobe, occipital lobe, and frontal lobe could be possible predictors for faster progression in patients with PD.

Previous studies have found that microstructural properties in the white matter and pallidum are associated with future motor and cognitive outcomes in patients with PD.[9,10,19] We found that microstructural properties of temporal lobe, occipital lobe, frontal lobe, and other subcortical regions apart from the pallidum were also correlated with the annual rate of changes in motor and nonmotor scores in PD. This is in line with previous finding that cortical microstructural properties are associated with clinical progression in preclinical Alzheimer disease.[11] Those regions with MD values associated with motor progression (i.e., UPDRS-Part-II and PIGD) were consistent with our previous finding that macrostructural measures (T1-weighted MRI derived) are associated with motor progression, which are primarily in subcortical regions.[39] However, there are more cortical regions with MD values associated with motor progression. One possible reason for the difference may be that microstructural changes detected by MD occur before macrostructural changes detected by T1-weighted MRI,[4,14] as Parkinson's pathology occurs in the subcortical regions before cortical regions.[2-4,6,32] Another possible interpretation is that macrostructural measures reflect brain resources, which can act as a resilience factor against clinical deterioration,[39,40] whereas microstructural changes detected by MD reflect pathologic changes. As gray matter volume loss is irreversible, our findings may have important clinical implications for disease-modifying therapies.

The biofluid levels of NfL are a sensitive biomarker of axonal damage and have shown to be a useful prognostic biomarker in PD.[16-18] We found a positive association between MD values and serum NfL levels, which further reinforces the notion that higher MD values reflect the underlying axonal neurodegeneration. The regions with MD values associated with serum NfL levels that partially overlapped with the result of a previous study[17] but further expanded to subcortical regions. In addition, R values derived from MD values and serum NfL levels were positively correlated with PAPs (eFigure 9, links.lww.com/WNL/C827). This indicates that those regions with high MD values are likely to relate with both high serum NfL levels and fast progression in PD. A common underlying factor might be neuroaxonal neurodegeneration. CSF α-synuclein levels were positively correlated with MD values of the right putamen, suggesting that α-synuclein aggregates are related to microstructural alteration of the putamen in PD.[3,4,6] Our results are in line with a previous study in which increased CSF α-synuclein predicted worsening of motor and cognitive progression.[41] We observed that CSF tau (i.e., p-tau181 and t-tau) levels were positively correlated with cortical MD values, but CSF $A\beta_{42}$ levels were negatively correlated with subcortical MD values. This connects well with previous findings that greater CSF p-tau181 and lower CSF Aβ42 at baseline predicted fast progression of motor and cognitive symptoms in PD,[42] and that tau facilitates α-synuclein aggregation and propagation in PD.[43]

Our enrichment analysis of CSF proteins associated with MD values found that the significant GO terms were primarily intracellular components or biological processes, which might reinforce the notion that higher MD values indicating cellular membrane damage releasing these intracellular components into CSF. Among these intracellular biological processes including mRNA metabolic process, DNA binding, mRNA processing, and regulation of mRNA splicing, consistent with a recent finding that α-synuclein modulates mRNA stability to regulate gene expression.[44] CSF proteins at bottom of the ordered list showed that significant GO terms were those involved in the biological processes of axon guidance and neuronal differentiation, suggesting that these processes may involve in protecting or repairing axonal or neuronal damage. In addition, the significant GO terms for bottom of the ordered CSF protein list also included glycoprotein metabolic process, transmembrane receptor tyrosine kinase activity, and Golgi membrane. These processes have been found to be related to Parkinson's pathology. For example, glycoprotein nonmetastatic melanoma protein B confers the risk for PD through interaction with α-synuclein.[45] Activation of the tyrosine kinase plays an essential role in the initiation and progression of α-synuclein pathology.[46] Fragmentation of the Golgi ribbon is a feature of PD.[47]

Finally, we discovered spatial concordance between PAPs and the receptor/transporter density maps of dopamine, glutamate, serotonin, cannabinoid, and GABA, suggesting microstructural changes in these regions that contain many of such neurons in healthy individuals. Dysregulation of the dopamine, glutamate, serotonin, cannabinoid, and GABA systems has been implicated in PD.[22,48] The density map of glutamate receptors was associated with both motor and nonmotor PAPs, suggesting that the glutamate neurotransmitter system is important for developing therapeutic drugs for PD.[49] Yet, ideally simultaneous PET and dMRI studies are needed to

provide a detailed insight into the mechanisms underlying this relationship. The density map of 5-HT_{1a} and CB1 was associated with nonmotor PAPs (i.e., UPDRS-I and MoCA), suggesting that these 2 neurotransmitter mapping patterns underlie microstructural alterations relating to nonmotor progression. This is consistent with the fact that mood and cognitive symptoms are often accompanied with abnormal serotonin or cannabinoid signaling.[5,34]

This study also has some limitations. First, this is a single cohort study, and the PPMI recruited patients with PD who were overwhelmingly White, generally highly educated, and younger than the general PD population, and as such, the PPMI dataset cannot be considered to be representative of the natural history of PD progression.[23] In addition, patients included in this study had shorter duration and less baseline disability than total enrolled patients with PD of the PPMI (eTable 3, links.lww.com/WNL/C827). Further study should be performed to validate the associations of microstructure in grey matter with clinical progression and fluid biomarkers in an independent PD cohort. Although free-water measures may provide better pathophysiologic information of PD progression, dMRI from PPMI was scanned with single shell (only B0 and B1000), which is not suited for free-water elimination DTI fitting.[50] Further study is needed to examine the relationship of free-water imaging measures and clinical progression with dMRI scanned with multishell acquisitions (need multiple *B* values between B0-B1000). Third, we observed a lower mean PIGD score at baseline than that of tremor. It is possible that a low mean score at baseline makes it easier to identify a change with time, and therefore, the annual rate of changes in PIGD was easier to be correlated with MD values. Fourth, the correlations between regional MD values with clinical progression and fluid biomarker levels come with the caveat that regional MD values are not independent measures. This indicates that regional MD values may not provide independent information about microstructural properties. Fifth, caution is required with respect to interpretation of observed associations of PAPs and spatial maps of neurotransmitter density because there are strong cross-correlations between different PET maps.[34] Sixth, the PET data were measured in generally younger, heathy volunteers, not in same patients scanned with dMRI and age-matched patients with PD.[50] Therefore, such analyses only reflected relationships between PAPs and the availability of specific receptors/transporters in younger, heathy volunteers, not relationships between PAPs and changes in the distribution of these transmitters between patients with PD and healthy controls. Finally, the CSF proteomics data are limited to subcellular localization of PD pathology, which should be investigated further.

In summary, we found that higher baseline cortical and subcortical MD values were associated with clinical progression and fluid biomarkers in PD, supporting the use of MD values for stratification of patients with different progression in the early stage of PD. Further longitudinal studies in different populations are needed to determine the prognostic utility of this noninvasive neuroimaging biomarker.

Acknowledgment

The authors thank all participants enrolled in this study.

Study Funding

J. Feng is supported by National Key R&D Program of China (No. 2019YFA0709502), Shanghai Municipal Science and Technology Major Project (No. 2018SHZDZX01), ZJ Lab, Shanghai Center for Brain Science and Brain-Inspired Technology, and the 111 Project (No. B18015). W. Cheng is supported by grants from the National Natural Science Foundation of China (No. 82071997) and the Shanghai Rising-Star Program (No. 21QA1408700). PPMI—a public-private partnership—is funded by the Michael J. Fox Foundation for Parkinson's Research funding partners 4D Pharma, AbbVie, Acurex Therapeutics, Allergan, Amathus Therapeutics, ASAP, Avid Radiopharmaceuticals, Bial Biotech, Biogen, BioLegend, Bristol-Myers Squibb, Calico, Celgene, DaCapo Brain Science, Denali, The Edmond J. Safra Foundation, GE HealthCare, Genentech, GlaxoSmithKline, Golub Capital, Handl Therapeutics, Insitro, Janssen Neuroscience, Lilly, Lundbeck, Merck, Meso Scale Discovery, Neurocrine Biosciences, Pfizer, Piramal, Prevail, Roche, Sanofi Genzyme, Servier, Takeda, Teva, UCB, Verily, and Voyager Therapeutics.

Disclosure

The authors report no disclosures relevant to this manuscript. Go to Neurology.org/N for full disclosures.

Publication History

Received by *Neurology* August 9, 2022. Accepted in final form March 28, 2023. Submitted and externally peer reviewed. The handling editor was Associate Editor Peter Hedera, MD, PhD.

Appendix Authors

Name	Location	Contribution
Linbo Wang, PhD	Institute of Science and Technology for Brain-Inspired Intelligence, Fudan University; Key Laboratory of Computational Neuroscience and Brain-Inspired Intelligence (Fudan University), Ministry of Education; MOE Frontiers Center for Brain Science, Fudan University; Zhangjiang Fudan International Innovation Center, Shanghai, China	Drafting/revision of the manuscript for content, including medical writing for content; study concept or design; and analysis or interpretation of data
Cheng Zhou, MD	Department of Radiology, The Second Affiliated Hospital, Zhejiang University School of Medicine, Hangzhou, China	Drafting/revision of the manuscript for content, including medical writing for content, and analysis or interpretation of data

Appendix *(continued)*

Name	Location	Contribution
Wei Zhang, MSc	Institute of Science and Technology for Brain-Inspired Intelligence, Fudan University; Key Laboratory of Computational Neuroscience and Brain-Inspired Intelligence (Fudan University), Ministry of Education; MOE Frontiers Center for Brain Science, Fudan University; Zhangjiang Fudan International Innovation Center, Shanghai, China	Drafting/revision of the manuscript for content, including medical writing for content; major role in the acquisition of data; and analysis or interpretation of data
Minming Zhang, MD	Department of Radiology, The Second Affiliated Hospital, Zhejiang University School of Medicine, Hangzhou, China	Drafting/revision of the manuscript for content, including medical writing for content; major role in the acquisition of data; and analysis or interpretation of data
Wei Cheng, PhD	Institute of Science and Technology for Brain-Inspired Intelligence, Fudan University; Key Laboratory of Computational Neuroscience and Brain-Inspired Intelligence (Fudan University), Ministry of Education; MOE Frontiers Center for Brain Science, Fudan University, Shanghai; Zhangjiang Fudan International Innovation Center, Shanghai, China; Fudan ISTBI—ZJNU Algorithm Centre for Brain-inspired Intelligence, Zhejiang Normal University, Jinhua, China	Drafting/revision of the manuscript for content, including medical writing for content; major role in the acquisition of data; study concept or design; and analysis or interpretation of data
Jianfeng Feng, PhD	Institute of Science and Technology for Brain-Inspired Intelligence, Fudan University; Key Laboratory of Computational Neuroscience and Brain-Inspired Intelligence (Fudan University), Ministry of Education; MOE Frontiers Center for Brain Science, Fudan University; Zhangjiang Fudan International Innovation Center, Shanghai, China; Department of Computer Science, University of Warwick, Coventry, United Kingdom	Drafting/revision of the manuscript for content, including medical writing for content; major role in the acquisition of data; study concept or design; and analysis or interpretation of data

References

1. Vázquez-Vélez GE, Zoghbi HY. Parkinson's disease genetics and pathophysiology. *Annu Rev Neurosci*. 2021;44(1):87-108. doi:10.1146/annurev-neuro-100720-034518
2. Lau A, So RWL, Lau HHC, et al. α-Synuclein strains target distinct brain regions and cell types. *Nat Neurosci*. 2020;23(1):21-31. doi:10.1038/s41593-019-0541-x
3. Chu Y, Morfini GA, Langhamer LB, He Y, Brady ST, Kordower JH. Alterations in axonal transport motor proteins in sporadic and experimental Parkinson's disease. *Brain*. 2012;135(7):2058-2073. doi:10.1093/brain/aws133
4. Rektor I, Svátková A, Vojtíšek L, et al. White matter alterations in Parkinson's disease with normal cognition precede grey matter atrophy. *PLoS One*. 2018;13(1):e0187939. doi:10.1371/journal.pone.0187939
5. Bloem BR, Okun MS, Klein C. Parkinson's disease. *Lancet*. 2021;397(10291):2284-2303. doi:10.1016/S0140-6736(21)00218-X
6. O'Keeffe GW, Sullivan AM. Evidence for dopaminergic axonal degeneration as an early pathological process in Parkinson's disease. *Park Relat Disord*. 2018;56:9-15. doi:10.1016/j.parkreldis.2018.06.025
7. Henderson MX, Cornblath EJ, Darwich A, et al. Spread of α-synuclein pathology through the brain connectome is modulated by selective vulnerability and predicted by network analysis. *Nat Neurosci*. 2019;22(8):1248-1257. doi:10.1038/s41593-019-0457-5
8. Aung WY, Mar S, Benzinger TL. Diffusion tensor MRI as a biomarker in axonal and myelin damage. *Imaging Med*. 2013;5:427-440. doi:10.2217/iim.13.49
9. Abbasi N, Fereshtehnejad SM, Zeighami Y, Larcher KMH, Postuma RB, Dagher A. Predicting severity and prognosis in Parkinson's disease from brain microstructure and connectivity. *NeuroImage Clin*. 2020;25:102111. doi:10.1016/j.nicl.2019.102111
10. Chung SJ, Kim YJ, Jung JH, et al. Association between white matter connectivity and early dementia in patients with Parkinson disease. *Neurology*. 2022;98(18):e1846-e1856. doi:10.1212/wnl.0000000000200152
11. Rodriguez-Vieitez E, Montal V, Sepulcre J, et al. Association of cortical microstructure with amyloid-β and tau: impact on cognitive decline, neurodegeneration, and clinical progression in older adults. *Mol Psychiatry*. 2021;26(12):7813-7822. doi:10.1038/s41380-021-01290-z
12. Ball G, Srinivasan L, Aljabar P, et al. Development of cortical microstructure in the preterm human brain. *Proc Natl Acad Sci USA*. 2013;110(23):9541-9546. doi:10.1073/pnas.1301652110
13. Taylor KI, Sambataro F, Boess F, Bertolino A, Dukart J. Progressive decline in gray and white matter integrity in de novo Parkinson's disease: an analysis of longitudinal Parkinson progression markers initiative diffusion tensor imaging data. *Front Aging Neurosci*. 2018;10:318. doi:10.3389/fnagi.2018.00318
14. Weston PSJ, Simpson IJA, Ryan NS, Ourselin S, Fox NC. Diffusion imaging changes in grey matter in Alzheimer's disease: a potential marker of early neurodegeneration. *Alzheimers Res Ther*. 2015;7(1):47. doi:10.1186/s13195-015-0132-3
15. Illán-Gala I, Montal V, Borrego-Écija S, et al. Cortical microstructure in the behavioural variant of frontotemporal dementia: looking beyond atrophy. *Brain*. 2019;142(4):1121-1133. doi:10.1093/brain/awz031
16. Bäckström D, Linder J, Jakobson Mo S, et al. NfL as a biomarker for neurodegeneration and survival in Parkinson disease. *Neurology*. 2020;95(7):e827-e838. doi:10.1212/wnl.0000000000010084
17. Sampedro F, Pérez-González R, Martínez-Horta S, Marín-Lahoz J, Pagonabarraga J, Kulisevsky J. Serum neurofilament light chain levels reflect cortical neurodegeneration in de novo Parkinson's disease. *Park Relat Disord*. 2020;74:43-49. doi:10.1016/j.parkreldis.2020.04.009
18. Lin CH, Li CH, Yang KC, et al. Blood NfL: a biomarker for disease severity and progression in Parkinson disease. *Neurology*. 2019;93(11):e1104-e1111. doi:10.1212/wnl.0000000000008088
19. Minett T, Su L, Mak E, et al. Longitudinal diffusion tensor imaging changes in early Parkinson's disease: ICICLE-PD study. *J Neurol*. 2018;265(7):1528-1539. doi:10.1007/s00415-018-8873-0
20. Oveisgharan S, Yu L, Poole VN, et al. Association of white matter hyperintensities with pathology and progression of parkinsonism in aging. *JAMA Neurol*. 2021;78(12):1494-1502. doi:10.1001/jamaneurol.2021.3996
21. Hsiao IT, Weng YH, Hsieh CJ, et al. Correlation of Parkinson disease severity and 18F-DTBZ positron emission tomography. *JAMA Neurol*. 2014;71(6):758-766. doi:10.1001/jamaneurol.2014.290
22. Barone P. Neurotransmission in Parkinson's disease: beyond dopamine. *Eur J Neurol*. 2010;17(3):364-376. doi:10.1111/j.1468-1331.2009.02900.x
23. Marek K, Chowdhury S, Siderowf A, et al. The Parkinson's Progression Markers Initiative (PPMI): establishing a PD biomarker cohort. *Ann Clin Transl Neurol*. 2018;5(12):1460-1477. doi:10.1002/acn3.644
24. Marek K, Jennings D, Lasch S, et al. The Parkinson Progression Marker Initiative (PPMI). *Prog Neurobiol*. 2011;95(4):629-635. doi:10.1016/j.pneurobio.2011.09.005
25. Goetz CG, Fahn S, Martinez-Martin P, et al. Movement Disorder Society-sponsored revision of the Unified Parkinson's Disease Rating Scale (MDS-UPDRS): process, format, and clinimetric testing plan. *Mov Disord*. 2007;22(1):41-47. doi:10.1002/mds.21198
26. Tomlinson CL, Stowe R, Patel S, Rick C, Gray R, Clarke CE. Systematic review of levodopa dose equivalency reporting in Parkinson's disease. *Mov Disord*. 2010;25(15):2649-2653. doi:10.1002/mds.23429
27. Dalrymple-Alford JC, MacAskill MR, Nakas CT, et al. The MoCA: well-suited screen for cognitive impairment in Parkinson disease. *Neurology*. 2010;75(19):1717-1725. doi:10.1212/wnl.0b013e3181fc29c9
28. Shapiro AM, Benedict RHB, Schretlen D, Brandt J. Construct and concurrent validity of the Hopkins Verbal Learning Test, Revised. *Clin Neuropsychol*. 1999;13(3):348-358. doi:10.1076/clin.13.3.348.1749
29. Forn C, Belloch V, Bustamante JC, et al. A Symbol Digit Modalities Test version suitable for functional MRI studies. *Neurosci Lett*. 2009;456(1):11-14. doi:10.1016/j.neulet.2009.03.081
30. Qualls CE, Bliwise NG, Stringer AY. Short forms of the Benton Judgment of Line Orientation Test: development and psychometric properties. *Arch Clin Neuropsychol*. 2000;15(2):159-163. doi:10.1093/arclin/15.2.159
31. Gladsjo JA, Schuman CC, Evans JD, Peavy GM, Miller SW, Heaton RK. Norms for letter and category fluency: demographic corrections for age, education, and ethnicity. *Assessment*. 1999;6(2):147-178. doi:10.1177/107319119900600204
32. Drori E, Berman S, Mezer AA. Mapping microstructural gradients of the human striatum in normal aging and Parkinson ' s disease. *Sci Adv*. 2022;8(28):eabm1971. doi:10.1126/sciadv.abm1971
33. Guttuso T, Sirica D, Tosun D, et al. Thalamic dorsomedial nucleus free water correlates with cognitive decline in Parkinson's disease. *Mov Disord*. 2022;37(3):490-501. doi:10.1002/mds.28886

34. Hansen JY, Shafiei G, Markello RD, et al. Mapping neurotransmitter systems to the structural and functional organization of the human neocortex. *Nat Neurosci*. 2022; 25(11):1569-1581. doi:10.1038/s41593-022-01186-3
35. Gold L, Ayers D, Bertino J, et al. Aptamer-based multiplexed proteomic technology for biomarker discovery. *PLoS One*. 2010;5(12):e15004. doi:10.1371/journal.pone.0015004
36. Johnson WE, Li C, Rabinovic A. Adjusting batch effects in microarray expression data using empirical Bayes methods. *Biostatistics*. 2007;8(1):118-127. doi:10.1093/biostatistics/kxj037
37. Subramanian A, Tamayo P, Mootha VK, et al. Gene set enrichment analysis: a knowledge-based approach for interpreting genome-wide expression profiles. *Proc Natl Acad Sci USA*. 2005;102(43):15545-15550. doi:10.1073/pnas.0506580102
38. Yu G, Wang LG, Han Y, He QY. ClusterProfiler: an R package for comparing biological themes among gene clusters. *Omi A J Integr Biol*. 2012;16(5):284-287. doi:10.1089/omi.2011.0118
39. Wang L, Wu P, Brown P, et al. Association of structural measurements of brain reserve with motor progression in patients with Parkinson disease. *Neurology*. 2022;99(10): E977-E988. doi:10.1212/wnl.0000000000200814
40. Gregory S, Long JD, Klöppel S, et al. Testing a longitudinal compensation model in premanifest Huntington's disease. *Brain*. 2018;141(7):2156-2166. doi:10.1093/brain/awy122
41. Hall S, Surova Y, Öhrfelt A, Zetterberg H, Lindqvist D, Hansson O. CSF biomarkers and clinical progression of Parkinson disease. *Neurology*. 2015;84(1):57-63. doi:10.1212/wnl.0000000000001098
42. Irwin DJ, Fedler J, Coffey CS, et al. Evolution of Alzheimer's disease cerebrospinal fluid biomarkers in early Parkinson's disease. *Ann Neurol*. 2020;88(3):574-587. doi:10.1002/ana.25811
43. Pan L, Li C, Meng L, et al. Tau accelerates α-synuclein aggregation and spreading in Parkinson's disease. *Brain*. 2022;145(10):3454-3471. doi:10.1093/brain/awac171
44. Hallacli E, Kayatekin C, NazeenWang SX, et al. The Parkinson's disease protein alpha-synuclein is a modulator of processing bodies and mRNA stability. *Cell*. 2022; 185(12):2035-2056.e33. doi:10.1016/j.cell.2022.05.008
45. Diaz-Ortiz ME, Seo Y, Posavi M, et al. GPNMB confers risk for Parkinson's disease through interaction with α-synuclein. *Science*. 2022;377(6608):eabk0637. doi:10.1126/science.abk0637
46. Werner MH, Olanow CW. Parkinson's disease modification through Abl kinase inhibition: an opportunity. *Mov Disord*. 2022;37(1):6-15. doi:10.1002/mds.28858
47. Fujita Y, Ohama E, Takatama M, Al-Sarraj S, Okamoto K. Fragmentation of Golgi apparatus of nigral neurons with α-synuclein-positive inclusions in patients with Parkinson's disease. *Acta Neuropathol*. 2006;112(3):261-265. doi:10.1007/s00401-006-0114-4
48. Cristino L, Bisogno T, Di Marzo V. Cannabinoids and the expanded endocannabinoid system in neurological disorders. *Nat Rev Neurol*. 2020;16(1):9-29. doi:10.1038/s41582-019-0284-z
49. Li X, Wang W, Yan J, Zeng F. Glutamic acid transporters: targets for neuroprotective therapies in Parkinson's disease. *Front Neurosci*. 2021;15:678154. doi:10.3389/fnins.2021.678154
50. Golub M, Neto Henriques R, Gouveia Nunes R. Free-water DTI estimates from single b-value data might seem plausible but must be interpreted with care. *Magn Reson Med*. 2021;85(5):2537-2551. doi:10.1002/mrm.28599

Association of Cortical and Subcortical Microstructure With Clinical Progression and Fluid Biomarkers in Patients With Parkinson Disease

Linbo Wang, Cheng Zhou, Wei Zhang, et al.

Neurology 2023;101;e300-e310 Published Online before print May 18, 2023
DOI 10.1212/WNL.0000000000207408